JOM, Vol. 66, No. 10, 2014
DOI: 10.1007/s11837-014-0997-9

Synthesis and Characterization of $CrCuFeMnMo_{0.5}Ti$ Multicomponent Alloy Bulks by Powder Metallurgy

KUIBAO ZHANG,[1,2] GUANJUN WEN,[1] HONGCHUAN DAI,[1] YUANCHENG TENG,[1] and YUXIANG LI[1]

1.—State Key Laboratory Cultivation Base for Nonmetal Composites and Functional Materials, Southwest University of Science and Technology, Mianyang 621010, China. 2.—e-mail: xiaobao320@163.com

In this study, $CrCuFeMnMo_{0.5}Ti$ multicomponent alloy bulks were prepared by powder metallurgy of mechanical alloying and sintering. A simple body-centered cubic (bcc) solid solution was prepared after 40 h ball milling of the raw $CrCuFeMnMo_{0.5}Ti$ metallic powder. Particles of the alloyed powder are in microsized structures, which are actually a soft agglomeration of lamellar grains with thicknesses less than 1 μm. Meanwhile, the lamellar granules are consisted of nanosized grains under rigid cold welding. The 80-h ball-milled powder was consolidated by cold pressing and subsequent sintering at 800°C. The observed main phase in the consolidated sample after milling for 80 h is still a bcc solid solution. The solidified sample of 80-h ball-milled powder exhibits a Vickers hardness of 468 HV, which is much higher than 171 HV of the counterpart prepared from the raw metallic powder.

INTRODUCTION

Multicomponent high-entropy alloys (HEAs), which contain at least five metallic elements with atomic percent between 5% and 35%, have attracted considerable attention from the scientific community since their evolution in 2004.[1–3] HEAs have broken the traditional alloy design concept based on one or two principal components.[4] The core principle behind HEAs is the use of high configurational entropy in the liquid state or regular solid-solution state, in which it has been suggested that it could lead to the formation of simple face-centered cubic (fcc), body-centered cubic (bcc), and/or hexagonal close-packed (hcp) solid solutions, nanosized precipitates, and even amorphous phases.[5–10] The distinctive structure and phase composition provide HEAs with multiple excellent properties, such as high strength, good ductility, and outstanding resistances to wear, oxidation, and corrosion.[6,11–15] The combination of excellent physical properties offers many potential engineering applications for HEAs, such as tools, molds, mechanical parts, etc.[16]

Until now, HEAs were prepared through many different techniques from primarily arc-melt casting,[1] to subsequent inductive melting,[7] spray coating,[3,17,18] powder metallurgy,[19–21] and electrochemical processes.[22] However, HEAs bulks fabricated by arc-melt or inductive-melt casting are limited in shape and size. Meanwhile, for some high-entropy alloy systems, elemental segregation has been observed during the melt casting process.[5,7,8] These shortcomings are great obstacles for the industrial application of HEAs. Powder metallurgy, which is considered as a low-cost and high-efficiency technique, is widely employed for the synthesis of nonequilibrium materials.[23] Not only new materials can be prepared by powder metallurgy, but also the properties of traditional materials can be promoted. From previous studies, HEA powders were readily obtained by mechanical alloying (MA) through adequate high-energy ball milling. The alloyed powders were subsequently consolidated by various methods to form bulky samples with the desired shape and dimension. It was reported that the solid solubility of mutual soluble components can be increased and supersaturated solid solutions can be prepared by MA.[24] For insoluble systems, alloys with a degree of solid solubility can be formed under high-energy collision. Thus, powder metallurgy is a promising technique not only for the basic research but also for the industrial application of HEAs.

To obtain the desired properties, the selection of HEA system is a very important consideration. Many HEA systems have been investigated from

(Published online June 7, 2014)

previous studies.[25] Al, Co, Cr, Cu, Fe, Mn, and Ti elements are mostly selected as matrix components. As Al exhibits a much larger atomic radius than other elements as shown in Table I, it is a disadvantage for the formation simple solid solutions.

Meanwhile, as Co is a strategic metal with a high price, it was not selected in this research. In the melt casting process of HEAs, Cu was considered as the initiator of phase separation.[5] But elemental separation would be ignored in the MA process.[23,24] Meanwhile, Mn exhibits similar atomic parameters as Cr, Cu, and Fe. Thus, Cr, Cu, Fe, and Mn were selected as the matrix components in this study. As Ti exhibits low solid solubility with these elements,[6,25] Ti was incorporated to explore the alloying behavior among these elements. Meanwhile, Mo was introduced as it was reported to be beneficial for the mechanical properties.[26,27] Eventually, CrCuFeMnMoTi was selected as the investigated alloy system with the elemental parameters listed in Table I. However, Mo demonstrates high electronegativity and a large atomic radius, which is not good for the formation of solid solution. Therefore, the atomic fraction of Mo is designed as 0.5 of the other elements. The multicomponent CrCuFeMnMo$_{0.5}$Ti bulky alloy was prepared by powder metallurgy from first conducting MA and subsequently performing sintering consolidation. The phase composition and microstructure evolution were investigated in this study. Alloying behavior and mechanical properties of the bulky alloys were explored as well.

EXPERIMENTAL DETAILS

Cr, Cu, Fe, Mn, Mo, and Ti elemental powders with purity higher than 98% and particle size smaller than 45 μm (325 mesh) were mixed and mechanically alloyed in a molar ratio of CrCuFeMnMo$_{0.5}$Ti. The MA process was carried out for up to 80 h in a high-energy planetary ball miller at 250 rpm with a ball-to-powder weight ratio of 15:1. High-performance stainless steel vials and balls were used as the milling media using *n*-heptane as the process-controlling agent (PCA). The powder samples were extracted at regular intervals of every 10 h during milling. The raw mixed powder and 80-h ball-milled powder were molded by cold pressing to form cylindrical pellets with diameter of 15 mm and height of 8 mm. The preformed specimens were subsequently sintered at 800°C for 2 h under flowing high-purity Ar atmosphere according to our previous research.[28] Phase compositions of the ball milled powder and sintered samples were characterized by Rigaku Ultima III x-ray diffractometer (XRD; Rigaku Corporation, Tokyo, Japan) with Cu Kα radiation. The microstructure of the milled powders and sintered samples were observed using scanning electron microscopy (SEM, Zeiss EVO-18; Carl Zeiss, Oberkochen, Germany). The chemical compositions were calculated from the results of an energy-dispersive x-ray spectrometer (EDX) equipped with field-emission scanning electron microscopy (FESEM; Zeiss Ultra-55). The thermal analyses were carried out at a NETZSCH STA 449C differential scanning calorimeter (DSC; NETZSCH Instruments, North America, LLC, Burlington, MA) under a heating rate of 10 K/min and flowing purified Ar atmosphere. The hardness measurements were conducted using a Vickers hardness tester (HV-1000A) under a load of 49 N for 15 s. At least seven tests were conducted to obtain the average values.

RESULTS AND DISCUSSIONS

X-ray Diffraction Analysis

CrCuFeMnMo$_{0.5}$Ti multicomponent alloy powder was ball milled from 10 h to 80 h with the x-ray diffraction patterns presented in Fig. 1a. To facilitate the analysis of XRD results, diffraction patterns located in the region of 38°–46° are magnified with the figure illustrated in Fig. 1b. It is shown that the raw mixed powder exhibits a diffraction pattern of all metallic elements. Mo and Ti are in overlapped XRD patterns with high intensity, whereas Cu, Fe, and Mn patterns are superimposed with much lower intensity. Diffraction intensity is related with many factors, such as atomic number, grain size, crystallinity, lattice strain, etc. For the raw powders of this alloy system, Mo is the heaviest element, which endows it with the highest XRD intensity. Drastic decrement of diffraction intensity is observed after 20 h of ball milling. The diffraction peaks of Cu, Fe, and Mn elements can hardly be identified after 40 h ball milling. At this time, only four diffraction peaks can be clearly observed. As the milling duration reaches up to 80 h, the

Table I. Atomic parameters of the experimental elements

Element	Cr	Cu	Fe	Mn	Mo	Ti
Atomic number	24	29	26	25	42	22
Melting point (°C)	1857	1083	1535	1244	2610	1668
Atom radius (10^{-12} m)	127	128	127	132	140	145
Electronic negativity	1.66	1.90	1.83	1.55	2.16	1.54
Crystal structure	bcc	fcc	bcc	bcc	bcc	hcp
Density (g/cm^3)	7.19	8.96	7.86	7.44	10.20	4.54

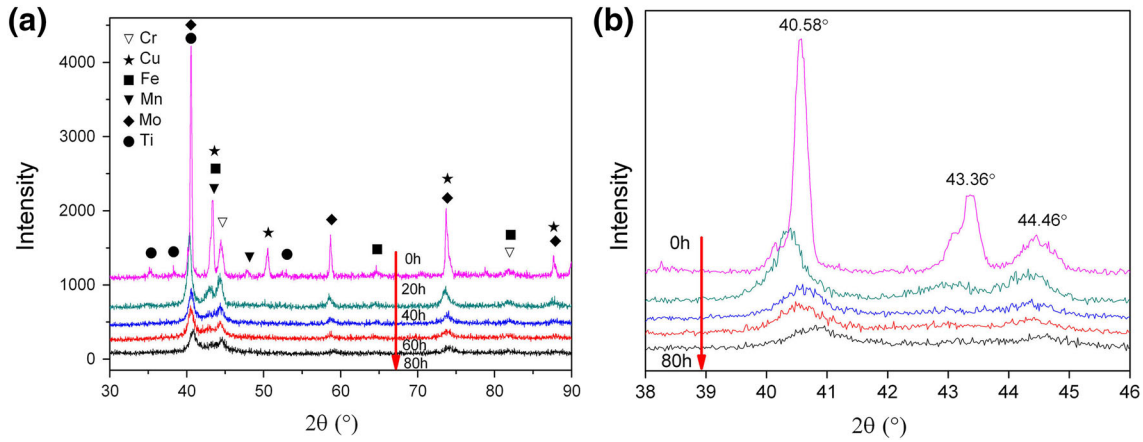

Fig. 1. (a) XRD patterns of $CrCuFeMnMo_{0.5}Ti$ multicomponent alloy powders under different milling durations and (b) magnified XRD patterns of (a) in the range of 38°–46°.

Table II. The crystalline size and lattice strain of $CrCuFeMnMo_{0.5}Ti$ multicomponent metallic powders under different milling duration

	$CrCuFeMnMo_{0.5}Ti$	
Milling time (h)	**Crystalline size (CS, nm)**	**Lattice strain (%)**
10	43.2	0.43
20	14.8	0.65
30	11.7	0.67
40	12.3	0.67
60	10.5	0.86
80	8.3	1.11

diffraction peaks exhibit no change except for a minor broadening. The disappearance of diffraction peaks and peak broadening can be considered as the beginning of solid-solution reaction.[24] The intensity decrement and peak broadening are related with the formation of nanocrystalline and high lattice strain induced by mechanical deformation during the MA process.[29]

The crystal size and lattice strain of the metallic powders under different milling durations have been calculated from the x-ray peak broadening using Scherrer's formula after eliminating the instrumental contribution (shown in Table II).

The crystalline size is greatly refined as the milling duration increases. The 80-h mechanically alloyed powder exhibits a crystal size of 8.3 nm. Refinement of the crystal structure is conducted by periodic crushment and cold welding during the milling process. This circulation invokes elemental diffusion and alloying, which eventually results in solid solutions for this multicomponent metallic powder. Alloying occurs when the grain sizes of the elemental components decrease down to nanometer range and a substantial amount of enthalpy can be stored in nanocrystalline alloys because of the large grain boundary area. The stored energy serves as the driving force for the production of solid solution.[29] Interdiffusion among the components occurs and the solid solubility is expected to be elevated as the milling time is prolonged. No further extension of solid solubility will be achieved until it reaches a supersaturation state.[24] The lattice strain of $CrCuFeMnMo_{0.5}Ti$ alloy powder increases gradually as the milling prolongs. The 80-h ball-milled powder exhibits a high lattice strain of 1.11%. Generally, the increment in lattice strain is caused by (I) the size mismatch effect among the constituents, (II) increased grain boundary fraction, and (III) mechanical deformation.[30] As the milling is extended, the grain boundary fraction and mechanical deformation are continuously increased because of the decreased grain size. The formation of solid solution among multiple elements increases the size mismatch because of their different atomic radius. The increment in lattice strain may also caused by the increased dislocation density produced by severe plastic deformation.[24]

Microstructure and Chemical Composition Characterization

Microstructures of the ball milled powders were characterized by scanning electron microscopy with the images illustrated in Fig. 2. Figure 2a shows the microstructure of the raw metallic powder, which contains all elemental powders with various particle sizes. The powders were obviously crushed down to refined particles with granular size less than 10 μm as it was ball milled for 20 h (Fig. 2b). In this process, the raw powders were first broken to form much smaller particles. The crushed granules were then cold welded to form much larger ones. This circulation of refinement and agglomeration continues for a long time. During this period, the particle size remains almost unchanged, whereas the grain size decreases continuously. Thus, a similar microstructure with slightly homogenized

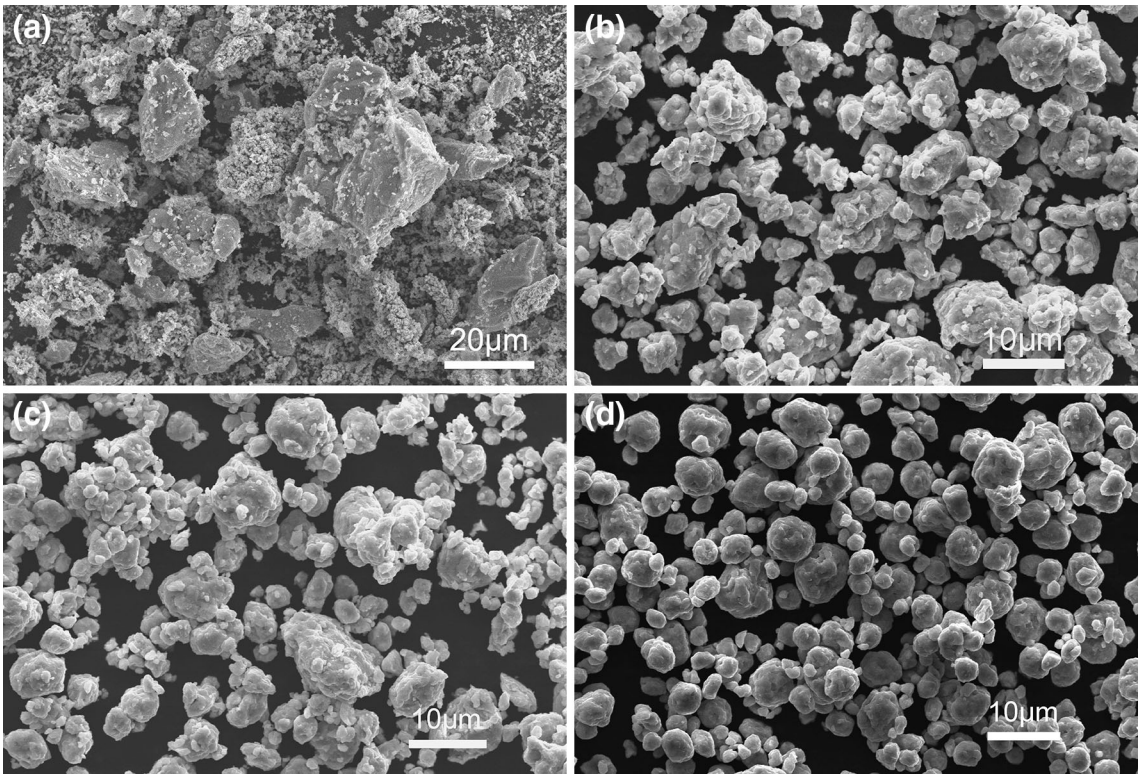

Fig. 2. SEM images of $CrCuFeMnMo_{0.5}Ti$ multicomponent metallic powders under different milling times: (a) 0 h, (b) 20 h, (c) 40 h, and (d) 60 h.

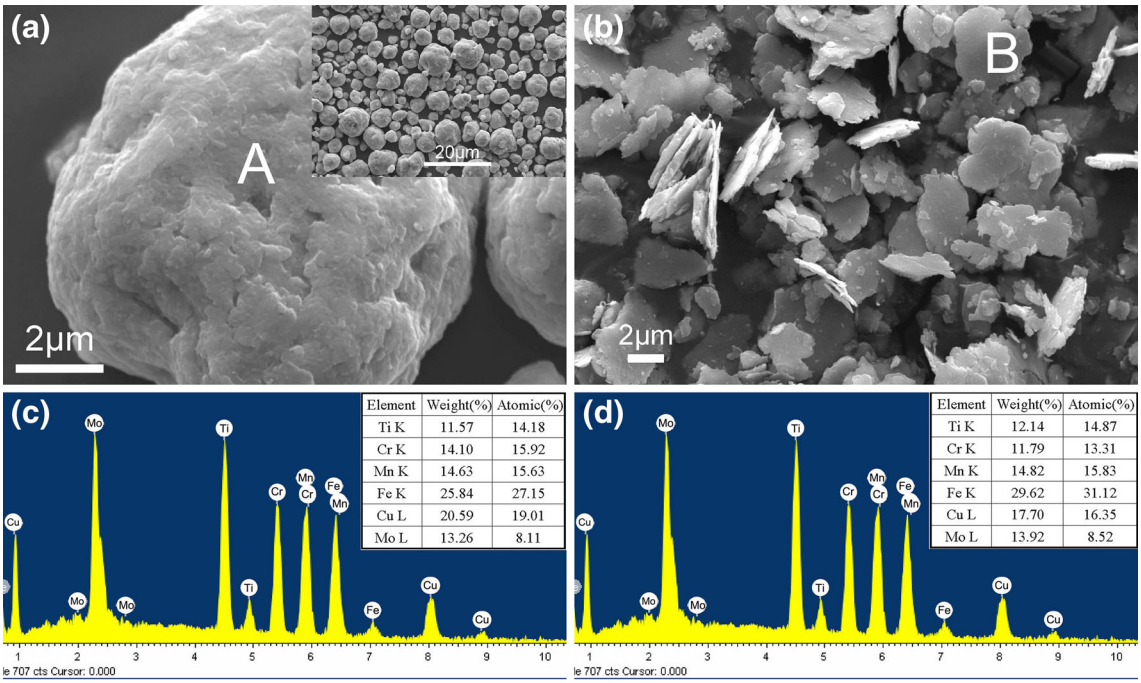

Fig. 3. SEM images and EDX analysis of $CrCuFeMnMo_{0.5}Ti$ multicomponent alloy powders: (a) 80 h milling, (b) 80 h dry milling + 2 h alcohol wet milling, (c) EDX result of (a), and (d) EDX result of (b).

particles can be observed in the 40-h ball-milled alloy powder as shown in Fig. 2c. However, the crystal size was refined from 14.8 nm to 12.3 nm according to Table I. The cycle of crushing and agglomeration continues as the milling prolongs, which makes the powder be refined gradually and

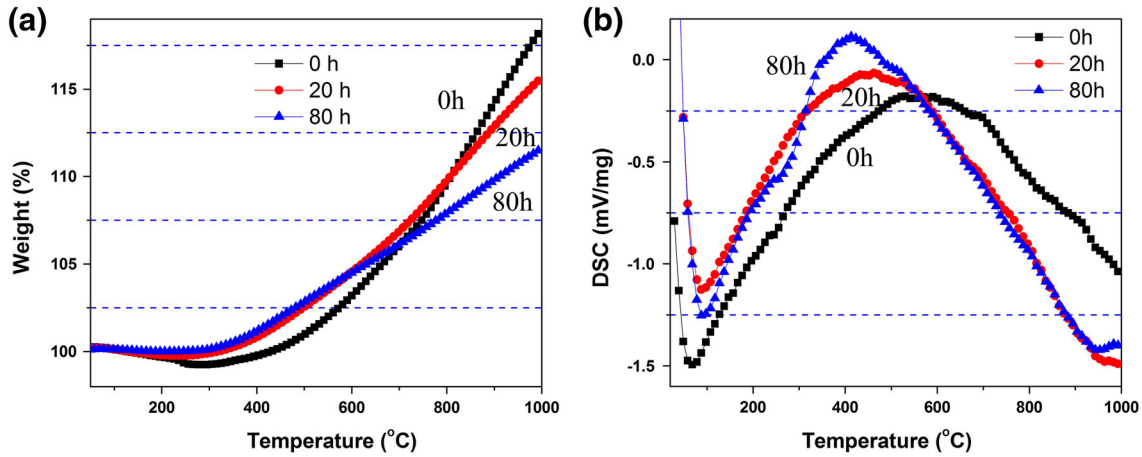

Fig. 4. Thermal analysis of 0 h, 20 h, and 60 h mechanically alloyed $CrCuFeMnMo_{0.5}Ti$ multicomponent alloy powders: (a) TG and (b) DSC curves.

facilitates the diffusion for alloying among different metallic elements. The 60-h ball-milled powder reveals an average particle size of about 5 μm as shown in Fig. 2d. The granules were further homogenized with near spherical shape.

As reported in previous studies.[20,28] prolonged milling of 60 h cannot further decrease the particle size. In this research, the milling duration was extended to 80 h as the microstructure presented in Fig. 3. The 80-h ball-milled powder shows similar morphology as the 60-h milled alloy powder with the morphology inserted in the upper-right corner of Fig. 3a. One large particle was selected to further examine the microstructure. It seems like this large particle is composed of many small granules. The elemental composition of the region labeled as A in this particle was measured by EDX with the result presented in Fig. 3c. All the metallic components exist in this particle. And their atomic amounts are equivalent to the designed elemental composition of $CrCuFeMnMo_{0.5}Ti$ except for Fe, which means the particle is composed of alloyed powder with all metallic components. To further illustrate microstructure of the 80-h ball-milled alloy powder, it was wet milled in alcohol for 2 h with the morphology presented in Fig. 3b. It can be observed that the wet-milled powders are in lamellar structure with thickness less than 1 μm. This means the dry-milled powders are actually an agglomeration of thin slices. The elemental composition of one slice labeled as B was calculated by EDX with the result presented in Fig. 3d. The lamellar exhibits similar elemental composition as the alloy particles in Fig. 3a. The Fe amount is also higher than the average value. This phenomenon indicates that the microsized thin slices are composed of nanoscaled crystals. These thin sheets pile up to form soft agglomeration of relatively larger elliptical-shaped particles. The EDX microanalysis results exhibit the chemical homogeneity and equivalent composition as designed after 80 h of ball milling.

Thermal Analysis of the Mechanically Alloyed Powders

Figure 4 shows the thermogravimetric (TG) and differential scanning calorimetry curves of 0-h, 20-h, and 80-h ball-milled metallic powders. The weight change of the alloy powders is presented in Fig. 4a. The powders exhibit a slight weight loss at the beginning of heat treatment with temperature lower than 300°C, which can be ascribed to the evaporation of moisture and PCA. After that, all powders demonstrate a trend of weight rising as the temperature is elevated. The weight gain is higher than 10 wt.% as the temperature increases to 1000°C. This phenomenon is associated with the surface oxidation as the protecting Ar gas is not pure enough. It is interesting that the 80-h milled powder exhibits much lower weight gain at 1000°C than the raw powder, which could indicate that the alloyed powders possess better oxidation resistance than the raw metallic powder.

Figure 4b reveals the calorimetry variations of 0-h, 20-h, and 80-h ball-milled alloy powders as the temperature increases to 1000°C. An abrupt endothermic peak exists at temperatures lower than 100°C, which can be attributed to water evaporation according to the TG result. There is a long exothermic line in the region of 100–950°C for all metallic powders. The peak release of energy increases as the milling duration prolonged and the 80-h milled alloy powder exhibits the most energy release. The energy fluctuation in this process can be related to the following four reasons:[20] (I) the reaction and evaporation of PCA, (II) the oxidation of metallic powder, (III) the release of internal stress, and (IV) phase transformation. For the raw powder, the exothermic peak is related only to the first two reasons while the mechanically alloyed powder may be related to all four reasons. There is a large amount of lattice strain in the ball milled powder, which will be released as the temperature increases.

Phase Composition and Vickers Hardness After Consolidation

The raw powder and 80-h mechanically alloyed powder were molded at 100 MPa by cold pressing. The preformed pellets were sintered at 800°C for 2 h in a tube furnace under flowing Ar atmosphere. Phase compositions of the consolidated samples were characterized by XRD with the resultant patterns demonstrated in Fig. 5. The XRD pattern of 80-h mechanically alloyed powder is incorporated for a comparison. XRD pattern of the bulky sample from raw metallic powder remains almost unchanged after forming and 800°C sintering. The diffraction peaks are coincident with the elementary metals of $CrCuFeMnMo_{0.5}Ti$, which reveals that 800°C sintering cannot evoke the alloying reaction for pure metals of this multicomponent alloy system. However, the feedback of 800 C sintering for 80-h ball-milled powder is totally different. It can be concluded from the XRD pattern that the main phase after sintering is multicomponent bcc solid solution. Besides, there are several intermetallic and complex phases, such as $Mo_5Cr_6Fe_{18}$, Fe_2TiO_5, and FeTi. Although the calcination was conducted under protection of flowing Ar atmosphere, the consolidated sample was slightly oxidized with an oxide product. The incorporation of oxygen is the result of surface adsorption in the milling procedure and impurity of the protecting Ar gas. Nevertheless, the main phase of the 80-h ball-milled and consolidated sample is bcc solid solution.

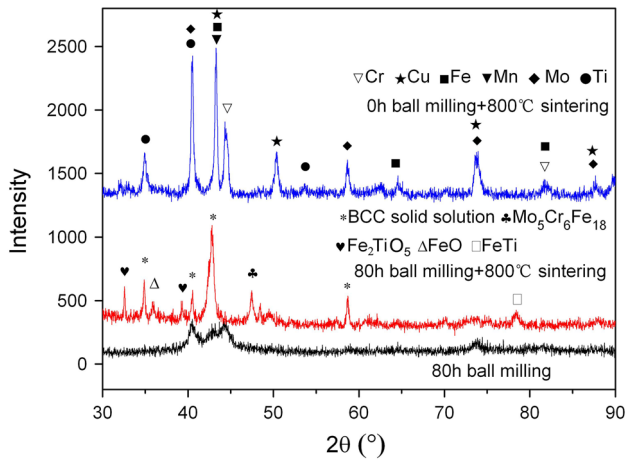

Fig. 5. XRD patterns of 800°C consolidated samples from raw powder and 80 h milled powder.

The consolidated samples from raw powder and 80-h mechanically alloyed powder were characterized by SEM with the surface morphology and corresponding EDX results illustrated in Fig. 6. The raw powder was highly densified after 2 h sintering at 800°C as shown in the backscattered SEM image in Fig. 6a. Elemental contrast can be observed in this image, which indicates the elemental distribution is not uniform. The elemental composition of the gray area labeled as "A" in Fig. 6a was analyzed by EDX with the resultant spectrum presented in Fig. 6c. The "A" particle is totally composed of Cr, which means no alloying reaction has taken place in the raw mixing powder after 800°C calcinations. This result is in accordance with the XRD pattern as

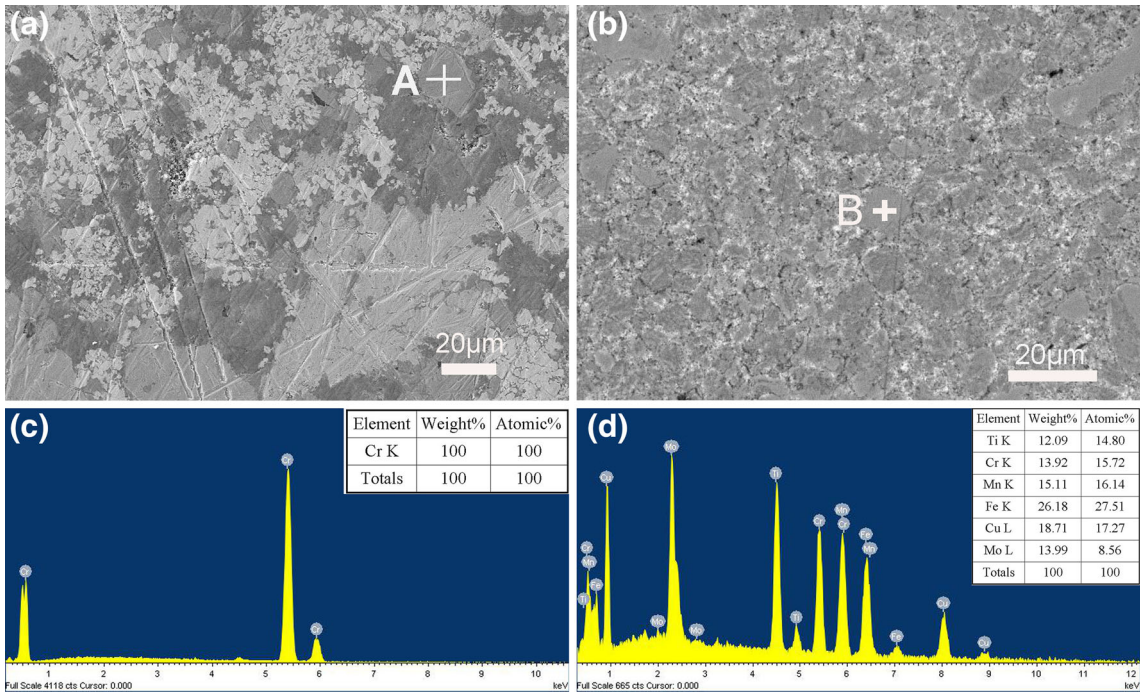

Fig. 6. SEM images and EDX analysis of consolidated $CrCuFeMnMo_{0.5}Ti$ multicomponent powders: (a) raw metallic powder, (b) 80-h milled alloy powder, (c) EDX result of (a), and (d) EDX result of (b).

illustrated in Fig. 5. The consolidated sample obtained from 80-h ball-milled powder also exhibits a highly densified surface structure as shown in Fig. 6b. The elemental contrast is not distinct in this image. Elemental composition of the grain labeled as "B" in Fig. 6b was characterized with the EDX result illustrated in Fig. 6d. It is shown that the "B" grain contains all elements of this alloy system, and their contents are very close to the mechanically alloyed powders as shown in Fig. 3. The Vickers hardness values of the consolidated samples from the raw powder and 80-h mechanically alloyed powder were readily measured. The mean value of the former sample is 171 HV. However, the pellet obtained from the 80-h ball-milled powder exhibits a mean Vickers hardness of 468 HV. The hardness improvement after MA is prominent. Powder metallurgy of preforming and sintering can realize this synthesis and maintain the property improvement.

CONCLUSION

$CrCuFeMnMo_{0.5}Ti$ multicomponent alloy bulks were successfully prepared by powder metallurgy in this study. The alloy powders, which are in simple BCC solid solution structure, were firstly synthesized by 80 h ball milling. Particles of the alloy powder are in near spherical structure with uniform size and elemental composition. The alloy particles are actually a soft agglomeration of lamellar grains with thickness less than 1 μm, which are composed of nanosized grains under rigid cold welding. The mechanically alloyed powder was subsequently consolidated by cold pressing and sintering in tube furnace at 800°C. The main phase of bcc solid solution was retained after heat treatment except for minor complex phases. The bulky sample prepared from the alloyed powder exhibits high Vickers hardness of 468 HV.

ACKNOWLEDGEMENTS

Dr. Kuibao Zhang sincerely appreciates financial support of the Open Project of State Key Laboratory Cultivation Base for Nonmetal Composites and Functional Materials (Southwest University of Science and Technology, No. 12zxfk15) and Doctoral Project of Southwest University of Science and Technology (No. 11zx7147).

REFERENCES

1. J.W. Yeh, S.K. Chen, S.J. Lin, J.Y. Gan, T.S. Chin, T.T. Shun, C.H. Tsau, and S.Y. Chang, *Adv. Eng. Mater.* 6, 299 (2004).
2. B. Cantor, I.T.H. Chang, P. Knight, and A.J.B. Vincent, *Mater. Sci. Eng. A* 375, 213 (2004).
3. T.K. Chen, T.T. Shun, J.W. Yeh, and M.S. Wong, *Surf. Coat. Technol.* 188, 193 (2004).
4. A.L. Greer, *Nature* 366, 303 (1993).
5. C.J. Tong, Y.L. Chen, J.W. Yeh, S.J. Lin, S.K. Chen, T.T. Shun, and C.H. Ts, *Metall. Mater. Trans. A* 36A, 881 (2005).
6. Y.J. Zhou, Y. Zhang, Y.L. Wang, and G.L. Chen, *Appl. Phys. Lett.* 90, 181904 (2007).
7. B.S. Li, Y.P. Wang, M.X. Ren, C. Yang, and H.Z. Fu, *Mater. Sci. Eng. A* 498, 482 (2008).
8. K.B. Zhang, Z.Y. Fu, J.Y. Zhang, W.M. Wang, H. Wang, Y.C. Wang, Q.J. Zhang, and J. Shi, *Mater. Sci. Eng. A* 508, 214 (2009).
9. S. Guo, Q. Hu, C. Ng, and C.T. Liu, *Intermetallics* 41, 96 (2013).
10. M.C. Gao and D.E. Alman, *Entropy* 15, 4504 (2013).
11. C.J. Tong, M.R. Chen, S.K. Chen, J.W. Yeh, T.T. Shun, S.J. Lin, and S.Y. Chang, *Metall. Mater. Trans. A* 36A, 1263 (2005).
12. X.F. Wang, Y. Zhang, Y. Qiao, and G.L. Chen, *Intermetallics* 15, 357 (2007).
13. Y.F. Kao, S.K. Chen, T.J. Chen, P.C. Chu, J.W. Yeh, and S.J. Lin, *J. Alloys Compd.* 509, 1607 (2011).
14. K.B. Zhang and Z.Y. Fu, *Intermetallics* 28, 34 (2012).
15. I. Kunce, M. Polanski, and J. Bystrzycki, *Int. J. Hydrog. Energy* 38, 12180 (2013).
16. J.W. Yeh, *Ann. Chim. Sci. Mater.* 31, 633 (2006).
17. Y.S. Huang, L. Chen, H.W. Lui, M.H. Cai, and J.W. Yeh, *Mater. Sci. Eng. A* 457, 77 (2007).
18. H. Zhang, Y. Pan, Y.Z. He, and H.S. Jiao, *Appl. Surf. Sci.* 257, 2259 (2011).
19. S. Varalakshmi, M. Kamaraj, and B.S. Murty, *J. Alloy. Compd.* 460, 253 (2008).
20. K.B. Zhang, Z.Y. Fu, J.Y. Zhang, W.M. Wang, S.W. Lee, and K. Niihara, *J. Alloy. Compd.* 485, L31 (2009).
21. Z.Q. Fu, W.P. Chen, H.Q. Xiao, L.W. Zhou, D.Z. Zhu, and S.F. Yang, *Mater. Des.* 44, 535 (2013).
22. C.Z. Yao, P. Zhang, M. Liu, G.R. Li, J.Q. Ye, P. Liu, and Y.X. Tong, *Electrochim. Acta* 53, 8359 (2008).
23. M.S. El-Eskandarany, *Mechanical Alloying for Fabrication of Advanced Engineering Materials* (New York: William Andrew Publishing, 2000).
24. C. Suryanarayana, *Prog. Mater. Sci.* 46, 1 (2001).
25. Y. Zhang, T.T. Zuo, Z. Tang, M.C. Gao, K.A. Dahmen, P.K. Liaw, and Z.P. Lu, *Prog. Mater. Sci.* 61, 1 (2014).
26. Y. Dong, Y.P. Lu, J.R. Kong, J.J. Zhang, and T.J. Li, *J. Alloy. Compd.* 573, 96 (2013).
27. C.Y. Hsu, C.C. Juan, W.R. Wang, T.S. Sheu, J.W. Yeh, and S.K. Chen, *Mater. Sci. Eng. A* 528, 3581 (2011).
28. K.B. Zhang, Z.Y. Fu, J.Y. Zhang, W.M. Wang, S.W. Lee, and K. Niihara, *J. Alloy. Compd.* 495, 33 (2010).
29. J.W. Yeh, S.Y. Chang, Y.D. Hong, S.K. Chen, and S.J. Lin, *Mater. Chem. Phys.* 103, 41 (2007).
30. J.Y. Huang, Y.D. Yu, Y.K. Wu, D.X. Li, and H.Q. Ye, *Acta Mater.* 45, 113 (1997).